

1 **The Future of Earth Imaging**

2

3 Victor C. Tsai

4 Department of Earth, Environmental and Planetary Sciences

5 Brown University, DEEPS, Box 1846

6 Providence RI, 02912, USA

7

8 **Abstract**

9 Imaging of Earth's interior has led to a large number of successful discoveries of plausible
10 structures and associated geophysical processes. However, due to the limitations of geophysical
11 data, Earth imaging has many tradeoffs between the underlying features, and most approaches
12 apply smoothing to reduce the effect of such tradeoffs. Unfortunately, this smoothing often
13 results in blurry images that are not clear enough either to infer the geologic processes of
14 interest or to make quantitative inferences about the various geologic properties. Here, we first
15 summarize some of the basic issues that make Earth imaging so difficult and explain how Earth
16 imagers must choose between more open-ended discovery oriented goals and more specific,
17 scientific inference oriented goals. We discuss how the choice of the optimal imaging
18 framework depends crucially on the desired goal, and particularly on whether plausible
19 discovery or inference is the desired outcome. We argue that as Earth imaging has become
20 more mature, sufficiently many plausible structures have been imaged that it is becoming more
21 crucial for Earth imaging to serve the inference goal and would benefit from an inference
22 oriented imaging framework, despite the additional challenges in posing imaging problems in
23 this manner. Examples of inference oriented imaging frameworks are provided and contrasted
24 with discovery oriented frameworks. We discuss how the success of the various frameworks
25 depends critically on the data quality and suggest that a careful balance must be struck
26 between the ambition of the imager and the reality of the data. If Earth imaging is to move
27 beyond presenting qualitatively plausible structures, it should move towards making
28 quantitative estimates of the underlying geologic processes, inferred through a self-consistent
29 framework.

30 **Introduction**

31 The inaccessibility of the Earth's interior has led to much speculation about its nature, including
32 many myths, science fiction stories, and scientific debates. Myths include the hell of Dante's
33 *Inferno* (Alighieri, 1472), or earthquake-causing subterranean turtles or catfish (SCEC, 2014;
34 Nur, 2008). Science fiction stories include Jules Verne's *Journey to the Center of the Earth*
35 (Verne, 1864), Lewis Carroll's *Alice in Wonderland* (Carroll, 1865), many other subterranean
36 world novels (Fitting, 2004), and the movie *The Core* (Amiel, 2003). More interesting from a
37 science perspective are the numerous scientific debates about the Earth's interior. These
38 include the 1690's-1930's debate over whether the Earth's interior was solid, fluid, gaseous or
39 hollow (Halley, 1692; Franklin, 1793; Brush, 1980), and the more recent debate about whether
40 narrow mantle plumes can be confirmed to exist or not (Montelli et al., 2004; van der Hilst and
41 de Hoop, 2005).

42

43 Due to its inaccessibility, many inferences about geophysical processes and the structure of
44 Earth's interior have come through imaging techniques, especially seismic imaging (e.g.,
45 Dziewonski and Anderson, 1981; Grand et al., 1997), but also imaging with other geophysical
46 data like gravity (Oldenburg, 1974), electromagnetic (Naif et al., 2013), muon (Tanaka et al.,
47 2009) and neutrino (Donini et al., 2019) data. The fact that the Earth has a core (Brush, 1980;
48 Muir & Tsai 2020a), that high-pressure mineral phases like Bridgmanite and Wadsleyite exist
49 (Ringwood & Major, 1966; Dziewonski & Anderson, 1981; Ringwood, 1991), and that
50 subducting plates likely impinge upon the lower mantle (Grand et al., 1997) have been
51 indicated primarily with seismic imaging.

52

53 However, despite the past successes of seismic imaging, there remain many debated
54 interpretations of seismic images, and it is often unclear from a science philosophy standpoint
55 whether certain Earth features claimed to be imaged are true beyond reasonable doubt, likely,
56 plausible, or simply false. As Earth imaging matures, we argue that insufficient attention has
57 been paid to the critical inference related aspects needed for such imaging to make a lasting
58 impact on our knowledge of the Earth's interior. We begin with a discussion of the critical
59 reasons that Earth imaging is challenging. While previous studies have commented on some of
60 the same issues of non-uniqueness and underdeterminism (e.g., Jackson, 1972; Zelt, 1999),
61 most studies still approach the problem within the standard discovery driven approach. Next,
62 we describe how imaging approaches can be framed as either being discovery oriented or
63 inference oriented and that these approaches have fundamentally different scientific
64 philosophies and goals. Finally, we describe some of the emerging ideas for posing inference
65 oriented Earth imaging and how they contrast with discovery oriented approaches.

66

67 **The Challenge of Earth Imaging**

68 Imaging is the use of observed data to produce a picture of the object of interest. In the case of
69 standard, light-based imaging, relatively high quality images are produced even with cheap
70 mobile phone cameras (see Fig. 1a). The success of standard imaging is well known (e.g., by
71 amateur photographers; Audubon, 2022) and can be attributed to the fact that (1) photons are
72 generally abundant, (2) the wavelength of visible light is relatively short (400-900 nanometers)
73 leading to sub-micron resolution, (3) air is minimally refractive so that photons usually travel

74 directly from the subject to the detector, and (4) modern cameras have millions of pixels that fit
75 easily into mm-sized semiconductor sensors. An example of such success is the photo of a cow
76 shown in Figure 1a, where it is clear that the subject is a cow. From an epistemological
77 standpoint, the viewer can have great confidence that the subject is a cow rather than a pig or a
78 walrus. Moreover, one can identify important characteristics of the cow, the relative sizes of
79 the cow's features can be measured quantitatively, and one could determine whether any
80 features are unexpected in size or shape.

81

82 Imaging also has many scientific applications (see Fig. 1). We can obtain detailed images of flow
83 in the interior of the sun (e.g., Fig. 1b, Gizon et al., 2010), we can image an 8-week human fetus
84 in utero the size of a peanut (Fig. 1c, Jauniaux et al., 2005), and we can even image the
85 structure of a single protein (Fig. 1d, Dubochet, 2018). In an Earth context, Figure 1e shows an
86 example seismic image that has been interpreted to show the subducted Farallon plate in the
87 lower mantle (Grand et al., 1997).

88

89 Perhaps surprisingly, in some ways it is more difficult to obtain clear images of the Earth's
90 interior than it is to image the sun's interior, the peanut-sized fetus or a single protein. Earth
91 imaging is difficult for the same considerations that make standard imaging easy. First, the
92 geophysical data that are most sensitive to the Earth's deep interior, namely seismic wave data,
93 are limited given the paucity of large enough seismic sources to illuminate regions of the Earth's
94 interior of interest. Second, the wavelength of seismic waves used is relatively long (10's-100's
95 of km), resulting in resolvable features of similar length scales for global (Hosseini et al., 2020)

96 and regional problems (Fichtner et al., 2009). Third, the Earth's interior is highly heterogeneous,
97 with geologic structures ranging from the micron to the hundreds-of-km scale that contribute
98 to significant refraction and reflection of seismic waves (Lay & Wallace, 1995). Finally, although
99 the number of sensitive, globally distributed seismic stations is impressive (e.g., Hosseini et al.,
100 2020), the few thousand broadband seismometers pales in comparison to the millions of
101 sensors in an iPhone camera, with major station coverage gaps in the oceans, Russia and Africa.
102 All of these reasons create tradeoffs that conspire to cause seismic images to be generally
103 blurrier than desired to make clear inferences about what structures exist in the Earth's interior
104 and what their characteristics are. Other geophysical data such as electromagnetic, gravity,
105 muon and neutrino data are even more limited than seismic data, and suffer many of the same
106 non-uniqueness problems. This explains why researchers have often struggled to use
107 geophysical imaging to go beyond suggesting that structures exist to clearly distinguishing
108 between different hypotheses about the existence and sizes of various structures and
109 geophysical processes.

110

111 **Discovery Versus Inference**

112 The dichotomy between the simultaneous success of Earth imaging in discovering plausible
113 features and yet the difficulty of using it to make clear inferences highlights the importance of
114 identifying its scientific purpose. Importantly, whether the result is successful or not depends
115 on the researcher's perspective and purpose, rather than there being an absolute metric of
116 success. Specifically, there is a significant difference between the goal of discovering plausible

117 features versus the goal of inferring specific characteristics (including about existence of
118 features).

119

120 A simple example helps demonstrate the difference between the ‘discovery’ and ‘inference’
121 goals. We return to the cow image (repeated in Fig. 2b) and ask whether Figure 2a (a blurry but
122 traditional photo) or Figure 2c (a cartoon cow impression with certain specific features
123 estimated) would be preferable if the ‘true’ Figure 2b were unavailable (setting aside for now
124 how these images would be obtained). The answer depends on one’s goal. If no prior
125 information were available and the purpose is to determine what is plausible, you may prefer
126 Figure 2a, where no assumptions were made about possible features. Although the image is
127 blurry, it is unbiased and has a wide range of possible outcomes, an advantage if one has no
128 idea what to expect. In contrast, if you know there is a cow and your purpose is to determine
129 the various cow features, you may prefer Figure 2c, where it is much clearer than from Figure
130 2a that the cow has 4 legs, 2 ears, spots, and even 4 teats on its udder and a red tag (all of
131 measurable sizes). This example underscores how the goal of unbiased discovery (or
132 exploration) of plausible structures is distinct from the goal of inferring specific characteristics
133 of a hypothesized object, and implies different preferences in approach. Interestingly, while
134 Figure 2b has 3.7 million pixels and thus 11.0 million parameters (RGB values), the number of
135 effective parameters needed for Figure 2a is about 2300 (smoothed \sim 70x) and only about 600
136 for Figure 2c (\sim 270 points plus colors). This is important if, for example, only 3000 pieces of
137 information were available. In this case, Figure 2b could not be produced, but Figure 2a and 2c
138 may be, depending on the structure of that information. Finally, we note that for Figure 2c, one

139 needs to propose a set of possible cow characteristics to test; using the wrong features would
140 lead either to no features or misinterpretations of other features.

141

142 This example highlights two related problems that plague scientific imaging and especially Earth
143 imaging, but which are not usually problems for traditional imaging. As already noted, Earth
144 imaging is data poor in that there is never enough data to constrain all details of geologic
145 structure that should exist in the Earth's interior. For example, geologic outcrops have
146 important structure at the sub-meter scale (Waldron & Snyder, 2020), and the Earth's volume is
147 approximately 10^{21} m^3 , meaning 10^{21} pieces of independent information (a zettabyte of
148 information) would be needed to determine Earth structure at a 1-meter resolution, an
149 impractical amount of data (equivalent to the global annual internet traffic). Even with a
150 growing amount of Earth data, Earth imagers will always be forced to make difficult decisions
151 about what features to focus on. Much like in the cow example with 3000 pieces of
152 information, the Earth imager simply cannot capture Figure 2b regardless of method, and must
153 embrace the strategy behind either Figure 2a, Figure 2c or some alternative that similarly uses
154 less than 3000 pieces of information. Thus, the choice between discovery-mode (Fig. 2a) and
155 inference-mode (Fig. 2c) approaches is apparent, and the Earth imager does not have the luxury
156 of avoiding the choice.

157

158 The fact that high-resolution Earth imaging problems have significant tradeoffs and are
159 therefore non-unique or underdetermined is well known (Jackson, 1972; Jordan, 1979) but, to
160 date, discovery-mode solutions to the Earth imaging problem have dominated. As elsewhere,

161 Earth imaging often uses pixels, grids, splines, spherical harmonics or other cell type structures
162 as the fundamental building blocks. These mathematical objects are chosen to be as general as
163 possible in order to accommodate the flexible discovery philosophy. Furthermore, in designing
164 the smoothing or regularization to reduce the number of effective parameters, there has
165 usually been a preference towards flexible mathematical regularization approaches. Tikhonov
166 regularization is one such common smoothing used in Earth imaging (Aster et al., 2013), and is a
167 good example of a very general approach to stabilizing an inversion that has too many grid cells
168 for a robust unregularized inversion. Tikhonov regularization results in the typical smoothing of
169 underdetermined images that is common, for example in Figure 1e. Other mathematical
170 approaches for addressing the same regularization problem can produce somewhat different
171 results, but still share the same philosophy regarding flexibility. For example, sparsity
172 regularization (e.g., Candes & Wakin, 2008), also known as compressive sensing, lasso or L1
173 regularization, is a recently popular alternative where fewer jumps in parameter values
174 between adjacent grid cells are preferred and used to effectively reduce the number of free
175 parameters. The underlying structure is otherwise unchanged, making sparsity regularization
176 useful when one expects a small number of sharp boundaries between discrete, homogeneous
177 objects but one still wants to maintain flexibility in the outcome. As such, sparsity regularization
178 takes a small step in the direction of interpretability for objects with sharp boundaries but
179 keeps most of the discovery philosophy. Similarly, other mathematical regularization
180 approaches, such as using large Voronoi cells to sample an ensemble of possible models
181 through a sub-space approach (Bodin & Sambridge, 2009), share the same philosophy and
182 accomplish a similar goal. A number of such mathematical approaches exist (e.g., Rudin et al.,

183 1992; Capdeville et al., 2010; Fichtner et al., 2021) and all fundamentally share the same
184 philosophy, while incorporating a small amount of a priori information.

185

186 The focus of Earth imaging on discovery and exploration was sensible, especially in the early
187 days of Earth imaging, when little was known about the Earth's interior. Discovery-mode Earth
188 imaging approaches have successfully led to a large number of Earth images with various
189 qualitative interpretations for what geologic structures exist and what their properties might
190 be. However, just like it is difficult to say anything quantitative using the blurry cow image in
191 Figure 2a, the vast majority of Earth image interpretations remain qualitative rather than
192 providing quantitative estimates either of the likelihood of correctness or of the physical
193 characteristics. Given the prior discussion, this is unsurprising, but this highlights the need for
194 Earth imaging to move in the direction of quantitative inference, particularly for regions that
195 already have discovery-mode images. Inference-mode imaging has a number of challenges that
196 discovery-mode imaging does not, including the difficulty of asking the right questions and the
197 extra technical expertise needed to correctly pose the problem and efficiently solve for the
198 important features (Tsai et al., 2023). But it is the only way in which Earth imaging will be able
199 to truly answer scientific questions posed about the appropriate geophysical processes
200 operating within the Earth. Thus, despite the challenges, it is time for Earth imagers to embrace
201 the inference philosophy more fully.

202

203 **Inference-Mode Imaging Approaches**

204 Just as there are a variety of discovery-mode approaches to Earth imaging, there have been a
205 number of suggested inference-mode approaches to Earth imaging, each with its pros and cons,
206 and some of which more completely embrace the inference goal than others. Many of these
207 approaches build upon discovery-mode approaches, including using them as starting points.
208 Here, we explain some of the differing approaches, with a focus on the differences in
209 philosophy and the implications for quantitatively answering geophysical questions.

210

211 ***Early examples of inference-mode imaging***

212 The idea that imaging can benefit from an inference framework is an old one that can be traced
213 back at least to the earliest experiments on the nature of light and specifically whether light is a
214 wave or a classical particle. Young's double-slit experiment (Young, 1804) was designed to test
215 whether the observed pattern would be the interference pattern predicted of the wave theory
216 or whether it would have the classically predicted two peak pattern. The goal of the imaging is
217 not to determine the detailed structure of the light pattern but rather to test between 2 very
218 specific hypotheses and determine which provides a better explanation of the observed data
219 (see Fig. 3).

220

221 This general idea has been used in Earth imaging, with Harold Jeffreys being one of the first to
222 clearly articulate (Jeffreys, 1939) what is now known as a Bayesian framework for how different
223 proposed models (with different parameter values) can be tested against observed geophysical
224 data. The general idea behind all such approaches is familiar to students of inverse theory in
225 that a prediction of each piece of data is made given a model framework and a range of

226 parameter values, and the model is preferred based on how closely the model predictions
227 (forward model) fit the observed data (Tarantola, 2005; Aster et al., 2013). Within a Bayesian
228 context, the data misfit provides a quantitative assessment for how reasonable the model is
229 and specifically the probability that the model is correct. When applied to model frameworks
230 with different parameters, this comparison between models is more difficult and requires use
231 of a model selection criterion to weigh the importance of accuracy versus simplicity (e.g.,
232 Sambridge et al., 2006), but otherwise has a similar philosophy.

233

234 Nataf & Ricard (1996) was one of the earliest studies to embrace a forward modeling
235 philosophy in whole Earth imaging problems, with a direct prediction of seismic wave speeds
236 using a geodynamical model. Unlike strictly Bayesian studies, they only computed the predicted
237 data for a single best-guess geodynamical model and declined to adjust the geodynamical
238 parameters to fit observed seismic data, but the idea was that their model could be used by
239 future imagers by doing so. Khan et al. (2008) took this concept one step farther, and into a
240 Bayesian framework, by directly estimating the mineralogy of the mantle using a comparison of
241 a seismic model (Dziewonski & Anderson, 1981) with an ensemble of predictions from mineral
242 physics models. This study was a significant conceptual step forward and suggested a different
243 mineralogy from what was commonly assumed, but limited in its comparison of strictly one-
244 dimensional (depth) structure, and therefore only average bulk properties of the Earth.
245 Koelemeijer et al. (2018) took this approach an additional step farther, testing seismic
246 predictions of three-dimensional geodynamical models with and without post-perovskite
247 directly against seismic tomographic images. The philosophy taken here is close to the

248 inference end-member discussed above. Unfortunately, a challenge of such an approach is
249 whether or not the model predictions can explore the full range of plausibly realistic models,
250 and whether the data are good enough to distinguish robustly between the numerous
251 possibilities or whether significant tradeoffs exist (see next section).

252

253 In a parallel line of research, Zelt (1999) pointed out that there are different strategies and
254 goals in imaging. Contrasting with the discovery-mode approach, he described what he called a
255 'minimum-parameter, prior-structure model' that includes strong prior information about what
256 physics or geometry exist, and in which imaging data is used to estimate a small number of
257 parameters related to these strong priors. This approach results in simple estimates of
258 geometric structures defined by prior ideas for what structures are reasonable. Similarly,
259 Magistrale et al. (2000) used various geophysical data including tomographic imaging data to
260 construct a simple rule-based model of seismic velocities in Southern California. In this work,
261 limitations on data availability necessitated the use of simple empirical constraints on
262 sedimentary basin velocities to construct a complete model across Southern California that
263 included such shallow basins. The resulting Southern California Earthquake Center (SCEC)
264 Community Velocity Model (CVM) Version 2 has been used by many researchers, but has since
265 been subsumed by more complex discovery-driven tomographic models like the SCEC CVM
266 Version 4.26 (Lee & Chen, 2016). While these early works of Zelt (1999) and Magistrale et al.
267 (2000) were simplistic in their assumed structures and ambitions, in many ways later work
268 described below builds upon the same philosophy but allowing for more sophisticated models
269 and hypotheses.

270

271 ***Recent examples of inference-mode earth imaging***

272 More recently, there has been a resurgence in the number of studies advocating for a variety of
273 different types of inference approaches to Earth imaging. We group these into 3 philosophically
274 distinct end-member contributions, which are exemplified by the works of Astic and Oldenburg
275 (2019), Arnold and Curtis (2018), and Tsai et al. (2023). Each of these involve inference as an
276 important principle and are archetypical of the range of modern approaches to inference-mode
277 imaging which are framed with modern data-quality constraints, available methodologies, and
278 uncertainty quantification. These emerging frameworks should help pave the road for future
279 inference-mode Earth imaging work.

280

281 The work of Astic and Oldenburg (2019) exemplifies a type of inference-based imaging in which
282 there are a small number of categories of structures with clearly distinct properties within an
283 arbitrarily complex spatial landscape. Their work demonstrates how 2 or 3 categories of known
284 (or modestly unknown) electrical conductivities can be determined from resistivity data more
285 robustly with a petrophysically and geologically guided inversion (PGI) compared with a
286 Tikhonov regularization approach. Importantly, this work is designed to offer maximum
287 flexibility regarding the spatial variability of the structures, using the data misfit and clustering
288 algorithms (e.g., Sun and Li, 2015) to converge close to a realistic geologic model. Other work
289 embraces a similar philosophy, though with different underlying methodologies and imaging
290 applications. For example, Linde et al. (2015) review how hydrogeological systems can be
291 categorized; Sun and Li (2015) demonstrate how to use gravity and crosswell seismic data to

292 identify distinct geologic units through clustering; Giraud et al. (2017) discuss how to use
293 geologic classification constraints to reduce the tradeoffs in gravity and magnetic inversions
294 through uncertainty estimation; and Muir and Tsai (2020b) show how seismic data can be used
295 to solve for geometrically distinct subsurface units using an Ensemble Kalman Inversion (EKI)
296 approach. Other similar applications are summarized by Moorkamp et al. (2016).

297

298 In their 'interrogation theory' framework, Arnold and Curtis (2018) take a different approach in
299 which they frame the entire geophysical imaging problem with a single overarching science
300 question that the imaging is designed to answer and which is 'interrogated' with the
301 geophysical imaging data. The philosophy taken is analogous to that of Young's double slit
302 experiment (see Fig. 3), where a single hypothesis is addressed and the imaging data is analyzed
303 only with respect to this hypothesis. Zhao et al. (2022) show how interrogation tomography can
304 be framed using different algorithms to answer the question 'What is the volume of a
305 subsurface body?' using seismic travel time data. The interrogation framework formalizes the
306 earlier approaches of Khan et al. (2008) and Koelemeijer et al. (2018). Those works could be
307 framed as asking the questions 'What is the average depth-dependent mineralogy of the
308 mantle?' and 'Does post-perovskite exist in the deep mantle?', respectively.

309

310 In yet another distinct approach to the inference problem, Tsai et al. (2023) advocate for
311 parametrizing imaging problems in terms of the geophysical processes and structures most
312 pertinent to the expected geologic setting, an approach they call 'geological tomography' (Fig.
313 4). They present a few examples of using idealized models of sedimentary basin formation,

314 subduction zone processes, and continental-scale architecture to directly parametrize models
315 for inverting seismic imaging data. This work intentionally reduces the flexibility of the possible
316 imaging results in favor of geologic interpretability of each parameter. A key feature and
317 simultaneous challenge is that the realisticness of the outcome depends on the quality of the
318 data and the modeling sophistication and ambition of the imager. Furthermore, due to the
319 different physical processes, data quality and a priori information, each application is expected
320 to require its own independent evaluation of how to pose the inference problem such that the
321 idealized model is commensurate with the data. In an analogy to the cow imaging problem, the
322 number of pieces of information and structural complexity of the cow cartoon should be
323 simpler when less information is available, and can be more realistic when more information is
324 available, as schematically shown in Figure 5a-e. This philosophy applies similarly to geological
325 tomography (subduction example in Fig. 5f-j; shallow subsurface example in Fig. 5k-o), not just
326 to features but also to the underlying geophysical processes and deformation which can be
327 included explicitly in the model parametrization if warranted. The geological tomography
328 framework formalizes the old but never fulfilled goal of Jordan (1979) of performing structural
329 geology of the global Earth's interior, and applies the 'simplifying, specific modeling' approach
330 discussed by van Zelst et al. (2022) to Earth imaging problems rather than the ad hoc geometric
331 approach of Zelt (1999). The philosophy is a pragmatic one that embodies the Einsteinian 'as
332 simple as possible, but not simpler' mantra (Dyson, 2004), with the result being explicit
333 quantitative estimates of exactly those physical parameters that the imager deems worthy of
334 investigation.

335

336 **Future Outlook for Inference-Mode Earth Imaging**

337 As Earth imaging moves beyond pure exploration and towards learning more precise
338 information about the Earth, it will be necessary for researchers to grapple with the challenges
339 of thinking about the purpose of imaging and how the framework used has important
340 implications for how successful the result will be in addressing the imager's goals. 'Discovery-
341 mode' imaging will always be useful in leading to hypotheses but 'inference-mode' frameworks
342 are crucial for robust discovery of hypothesized features, e.g., as used classically by Young to
343 discover the wave nature of light (Fig. 3) and also by Le Verrier (1846) to discover the planet
344 Neptune. Given the recent frameworks exemplified by Astic and Oldenburg (2019), Arnold and
345 Curtis (2018) and Tsai et al. (2023), the Earth imaging field is well prepared to take the next
346 steps towards inference. These and other recent inference oriented imaging studies have just
347 scratched the surface in terms of possible applications, but a set of possible directions has been
348 set for the Earth imaging community to follow. While inference-mode imaging has many
349 technical challenges that traditional imaging does not (e.g., Tsai et al., 2023) and can easily be
350 biased by the use of non-independent data (a form of data dredging), it is exciting to see the
351 field mature to the point where robust conclusions about the mysteries of the Earth's interior
352 may finally see the light of day. Whether we reach this point may be a matter of whether we, as
353 a community, have the ambition, patience and education to follow this challenging path.

354

355 **Data and Resources**

356 No data were used in this paper.

357

358 **Declaration of Competing Interests**

359 The author declares no competing interests.

360

361 **Acknowledgments**

362 The author thanks the US Department of Agriculture, Laurent Gizon, Pulin Li and Alden Tsai,

363 Seychelle Vos, and Suzan van der Lee for graciously providing the images in Figure 1; Daniel

364 Bowden, Colleen Dalton and Andreas Fichtner for helpful suggestions; and editor Allison Bent

365 for shepherding this paper through review. This work was partially supported by NSF grant EAR-

366 2011079.

367

368 **References**

369 Alighieri, D. (1472). *La Comedia di Dante Alleghieri*, Johann Numeister and Evangelista Angelini

370 da Trevi, Foligno.

371 Amiel, J. (Director) (2003). *The Core* [Film], David Foster Productions.

372 Arnold, R., and A. Curtis (2018). Interrogation theory, *Geophys. J. Int.* 214, 1830-1846.

373 Aster, R.C., B. Borchers, and C.H. Thurber (2013). *Parameter Estimation and Inverse Problems*,

374 Elsevier, New York, 2nd edition.

375 Astic, T., and D.W. Oldenburg (2019). A framework for petrophysically and geologically guided

376 geophysical inversion using a dynamic Gaussian mixture model prior, *Geophys. J. Int.* 219,

377 1989-2012.

378 Audubon (2022). *The 2022 Audubon Photography Awards: The Top 100*.

379 <https://www.audubon.org/news/the-2022-audubon-photography-awards-top-100>

380 Bodin, T., and M. Sambridge (2009). Seismic tomography with the reversible jump algorithm,
381 *Geophys. J. Int.* 178, 1411-1436.

382 Bourgeois, A., M. Bourget, P. Lailly, M. Poulet, P. Ricarte, and R. Versteeg (1990). Marmousi,
383 model and data, *EAEG workshop-practical aspects of seismic data inversion*, cp-108-00002,
384 EAGE publications, May 1990.

385 Brush, S.G. (1980). Discovery of the Earth's core, *Am. J. Phys.* 48, 705-724.

386 Candes, E.J., and M.B. Wakin (2008). An introduction to compressive sampling, *IEEE Signal
387 Process. Mag.*, Mar 2008, 21-38, doi:10.1109/MSP.2007.914731.

388 Capdeville, Y., L. Guillot, and J.-J. Marigo (2010). 2-D non-periodic homogenization to upscale
389 elastic media for P-SV waves, *Geophys. J. Int.* 182, 903-922.

390 Carroll, L. (1865). *Alice's Adventures in Wonderland*, Macmillan Publishers, London.

391 Donini, A., S. Palomares-Ruiz, and J. Salvado (2019). Neutrino tomography of Earth, *Nature
392 Phys.* 15, 37-40.

393 Dubochet, J. (2018). On the development of electron cryo-microscopy (Nobel lecture), *Angew.
394 Chem. Int. Ed.* 57, 10842-10846.

395 Dyson, F. (2004). A meeting with Enrico Fermi, *Nature* 427, 297.

396 Dziewonski, A.M., and D.L. Anderson (1981). Preliminary reference Earth model, *Phys. Earth
397 Planet. Int.* 25, 297-356.

398 Fichtner, A., B.L.N. Kennett, H. Igel, and H.-P. Bunge (2009). Full seismic waveform tomography
399 for upper-mantle structure in the Australasian region using adjoint methods, *Geophys. J. Int.*
400 179, 1703-1725.

401 Fichtner, A., A. Zunino, L. Gebraad, and C. Boehm (2021). Autotuning Hamiltonian Monte Carlo
402 for efficient generalized nullspace exploration, *Geophys. J. Int.*, 227, 941-968.

403 Fitting, P. (2004). *Subterranean Worlds: A critical anthology*, Wesleyan University Press,
404 Middletown.

405 Franklin, B. (1793). Queries and conjectures relative to magnetism, and the theory of the Earth,
406 in a letter from Dr. B. Franklin, to Mr. Bodoin, *Trans. Am. Phil. Soc.* 3, 10-13.

407 Grand, S.P., R.D. van der Hilst, and S. Widjayanoro (1997). Global seismic tomography: A
408 snapshot of convection in the Earth, *GSA Today* 7, 1-6.

409 Halley, E. (1692). An account of the cause of the change of the variation of the magnetic needle;
410 with an hypothesis of the structure of the internal parts of the Earth, *Phil. Trans. Royal Soc.*
411 *Lond.* 195, 563-578.

412 Hosseini, K., K. Sigloch, M. Tsekhmistrenko, A. Zaheri, T. Nissen-Meyer, and H. Igel (2020).
413 Global mantle structure from multifrequency tomography using P, PP and P-diffracted
414 waves, *Geophys. J. Int.* 220, 96-141.

415 Jackson, D.D. (1972). Interpretation of inaccurate, insufficient and inconsistent data, *Geophys. J.*
416 *R. Astr. Soc.* 28, 97-109.

417 Jauniaux, E., J. Johns, and G.J. Burton (2005). The role of ultrasound imaging in diagnosing and
418 investigating early pregnancy failure, *Ultrasound Obstet. Gynecol.* 25, 613-624.

419 Jeffreys, H. (1939). *Theory of Probability*, Oxford University Press, Oxford, 1st edition.

420 Jordan, T.H. (1979). Structural geology of the Earth's interior, *Proc. Natl. Acad. Sci.* 76, 4192-
421 4200.

422 Koelemeijer, P., B.S.A. Schuberth, D.R. Davies, A. Deuss, and J. Ritsema (2018). Constraints on
423 the presence of post-perovskite in Earth's lowermost mantle from tomographic-geodynamic
424 model comparisons, *Earth Planet. Sci. Lett.* 494, 226-238.

425 Khan, A., J.A.D. Connolly, and S.R. Taylor (2008). Inversion of seismic and geodetic data for the
426 major element chemistry and temperature of the Earth's mantle, *J. Geophys. Res.* 113,
427 B09308, doi:10.1029/2007JB005239.

428 Lay, T., and T.C. Wallace (1995). *Modern Global Seismology*, Academic Press, San Diego.

429 Le Verrier, U.-J. (1846). Recherches sur les mouvements d'Uranus, *Les Comptes Rendus de*
430 *l'Academie des Sciences* 22, 907-918.

431 Lee, E.-J., and P. Chen (2016). Improved basin structures in Southern California obtained
432 through full-3D seismic waveform tomography (F3DT), *Seismol. Res. Lett.* 87, 874-881.

433 Magistrale, H., S. Day, R.W. Clayton, and R. Graves (2000). The SCEC southern California
434 reference three-dimensional seismic velocity model version 2, *Bull. Seismol. Soc. Am.* 90,
435 S65-S76.

436 Montelli, R., G. Nolet, F.A. Dahlen, G. Masters, E.R. Engdahl, and S.-H. Hung (2004). Finite-
437 frequency tomography reveals a variety of plumes in the mantle, *Science* 303, 338-343.

438 Moorkamp, M., P.G. Lelievre, N. Linde, and A. Khan (2016). *Integrated Imaging of the Earth:*
439 *Theory and Applications*, Vol. 218, John Wiley and Sons.

440 Muir, J.B., and V.C. Tsai (2020a). Did Oldham discover the core after all? Handling imprecise
441 historical data with hierarchical Bayesian model selection, *Seismol. Res. Lett.* 91, 1377-1383.

442 Muir, J.B., and V.C. Tsai (2020b). Geometric and level set tomography using ensemble Kalman
443 inversion, *Geophys. J. Int.* 220, 967-980, doi:10.1093/gji/ggz472.

444 Naif, S., K. Key, S. Constable, and R.L. Evans (2013). Melt-rich channel observed at the
445 lithosphere-asthenosphere boundary, *Nature* 495, 356-359.

446 Nataf, H.-C., and Y. Ricard (1996). 3SMAC: an a priori tomographic model of the upper mantle
447 based on geophysical modeling, *Phys. Earth Planet. Inter.* 95, 101-122.

448 Nur, A. (with Burgess, D.) (2008). *Apocalypse: Earthquakes, Archaeology, and the Wrath of God*,
449 Princeton University Press, Princeton.

450 Oldenburg, D.W. (1974). The inversion and interpretation of gravity anomalies, *Geophys.* 39,
451 526-536.

452 Ringwood, A.E. (1991). Phase transformations and their bearing on the constitution and
453 dynamics of the mantle, *Geochim. Cosmochim. Acta* 55, 2083-2110.

454 Ringwood, A.E., and A. Major (1966). High-pressure transformations in pyroxenes, *Earth Planet.*
455 *Sci. Lett.* 1, 351-357.

456 Rudin, L.I., S. Osher, and E. Fatemi (1992). Nonlinear total variation based noise removal
457 algorithms, *Physica D* 60, 259-268.

458 Sambridge, M., K. Gallagher, A. Jackson, and P. Rickwood (2006). Trans-dimensional inverse
459 problems, model comparison and the evidence, *Geophys. J. Int.* 167, 528-542.

460 SCEC, 2014. The turtle story, a native American account of earthquakes. *YouTube*, uploaded by
461 SCEC, 10 Jan 2014, https://www.youtube.com/watch?v=8_83ppaxT74.

462 Tanaka, H.K.M., T. Uchida, M. Tanaka, H. Shinohara, and H. Taira (2009). Cosmic-ray muon
463 imaging of magma in a conduit: degassing process of Satsuma-Iwojima Volcano, Japan,
464 *Geophys. Res. Lett.* 36, L01304.

465 Tarantola, A. (2005). *Inverse Problem Theory and Methods for Model Parameter Estimation*,
466 SIAM.

467 Tsai, V.C., C. Huber, and C.A. Dalton (2023). Towards the geological parametrization of seismic
468 tomography, *Geophys. J. Int.* 234, 1447-1462, doi:10.1093/gji/ggad140.

469 van der Hilst, R.D., and M.V. de Hoop (2005). Banana-doughnut kernels and mantle
470 tomography, *Geophys. J. Int.* 163, 956-961.

471 van Zelst, I., F. Crameri, A.E. Pusok, A. Glerum, J. Dannberg, and C. Thieulot (2022). 101
472 geodynamic modelling: how to design, interpret, and communicate numerical studies of the
473 solid Earth, *Solid Earth* 13, 583-637.

474 Verne, J. (1864). *Voyage au Centre de la Terre*, J. Hetzel et Cie, Paris.

475 Waldron, J., and M. Snyder (2020). *Geological structures: A practical introduction*, University of
476 Alberta, Alberta. <https://openeducationalalberta.ca/introductorystructuralgeology/>

477 Young, T. (1804). The Bakerian lecture. Experiments and calculation relative to physical optics,
478 *Phil. Trans. Royal Soc. London* 94, 1-16.

479 Zelt, C.A. (1999). Modelling strategies and model assessment for wide-angle seismic travelttime
480 data, *Geophys. J. Int.* 139, 183-204.

481 Zhao, X., A. Curtis, and X. Zhang (2022). Interrogating subsurface structures using probabilistic
482 tomography: an example assessing the volume of the Irish Sea basins, *J. Geophys. Res.* 127,
483 e2022JB024098.

484

485 **Full Mailing Address for Each Author**

486 Victor C. Tsai

487 Department of Earth, Environmental and Planetary Sciences

488 Brown University, DEEPS, Box 1846

489 Providence RI, 02912, USA

490

491 **Figure Captions**

492 **Figure 1.** Five imaging examples at different scales. (a) An image of a cow taken with a cheap
493 standard camera. (b) An image of the sun from helioseismic Doppler imaging (colors denote
494 magnetic field strength, arrows denote horizontal velocities up to 300 m/s). (c) Fetal ultrasound
495 image showing a live 8-week fetus (~1 cm) plus yolk sac (~3 mm) within the uterus. (d) Image of
496 an RNA polymerase protein reconstructed using cryo-electron microscopy. (e) Image of the
497 subducted Farallon plate underneath North America from seismic data. Images from (a)
498 reprinted from ars.usda.gov/oc/images/photos/k5176-3/, (b) reprinted from arXiv:1001.0930
499 and courtesy of Laurent Gizon, (c) courtesy of the author, (d) courtesy of Seychelle Vos, (e)
500 courtesy of Suzan van der Lee.

501

502 **Figure 2.** Comparison of different approaches to imaging. (b) represents the truth and contains
503 11.0 million pieces of information (assumed unavailable in the example). (a) is a version of (b)
504 that is blurry due to smoothing by a factor of 70 in both directions, resulting in ~2300 pieces of
505 information. (c) is an image constructed out of cow features (head, udder, legs, spots, eyes,
506 ears, tag) and uses ~600 pieces of information. The smoothed image in (a) is most useful in
507 discovery mode. The featured image in (c) is most useful in inference mode.

508

509 **Figure 3.** Young's double slit experiment with 2 distinct imaging hypotheses. (a) The classical
510 theory predicts 2 lines. (b) The wave theory predicts a central peak and a large number of
511 adjacent lines of different intensities depending on the wavelength. The purpose of the
512 experiment is to test the 2 specific hypotheses.

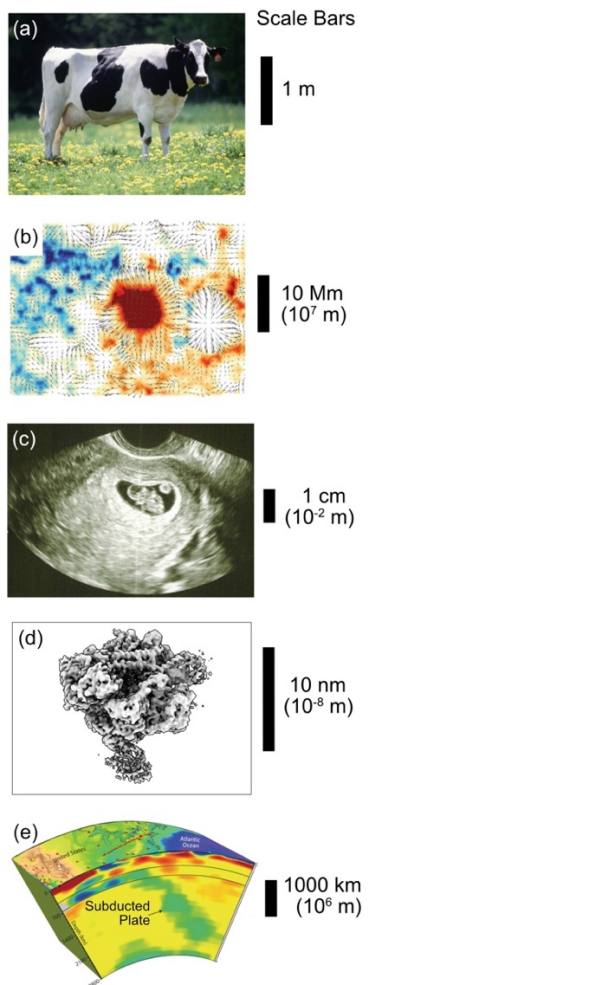
513

514 **Figure 4.** Example geologic parametrizations for imaging. (a) Example sedimentary basin
515 parametrization with 14 parameters, characterizing 2 graben forming and 2 deposition geologic
516 events. (b) Example subduction zone parametrization with 8 parameters, including cooling of
517 the mantle wedge by the subducting plate. Adapted from Tsai et al. (2023).

518

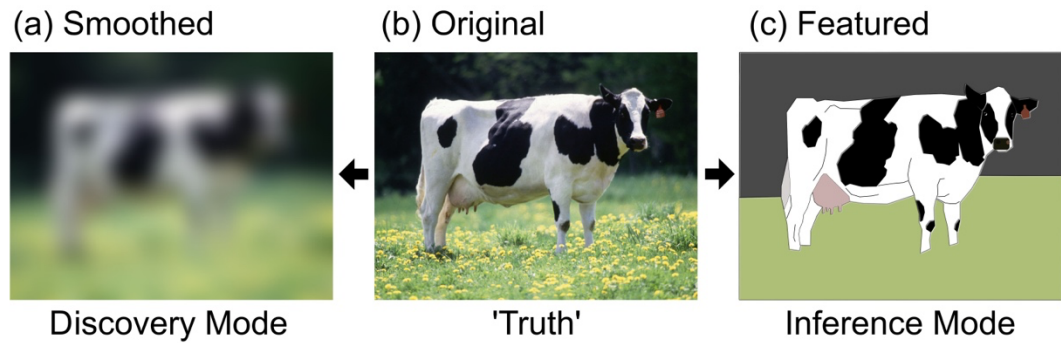
519 **Figure 5.** Schematic showing how models of a cow (a-e), a subduction zone (f-j) and a shallow
520 subsurface structure (k-o) can be simpler or more realistic and encode less information or more
521 information, respectively. The approximate number of pieces of information required to
522 produce the cartoon in each panel is provided below each image. (a) A 'spherical cow' cartoon.
523 (b-d) Intermediate complexity cartoon cows. (e) A realistic cartoon cow that approximates the
524 cow in Fig. 2b. The geologic models in (f-o) are not just composed of arbitrary geometric objects
525 but instead represent various geophysical processes and assumed deformation rules when used
526 for 'geological tomography'. Structure in (k-o) inspired by the Marmousi model (Bourgeois et
527 al., 1990).

528



529

530 **Figure 1.** Five imaging examples at different scales. (a) An image of a cow taken with a cheap
 531 standard camera. (b) An image of the sun from helioseismic Doppler imaging (colors denote
 532 magnetic field strength, arrows denote horizontal velocities up to 300 m/s). (c) Fetal ultrasound
 533 image showing a live 8-week fetus (~1 cm) plus yolk sac (~3 mm) within the uterus. (d) Image of
 534 an RNA polymerase protein reconstructed using cryo-electron microscopy. (e) Image of the
 535 subducted Farallon plate underneath North America from seismic data. Images from (a)
 536 reprinted from ars.usda.gov/oc/images/photos/k5176-3/, (b) reprinted from [arXiv:1001.0930](https://arxiv.org/abs/1001.0930)
 537 and courtesy of Laurent Gizon, (c) courtesy of the author, (d) courtesy of Seychelle Vos, (e)
 538 courtesy of Suzan van der Lee.



539 Pieces of
information:

~2300

~11.0 million

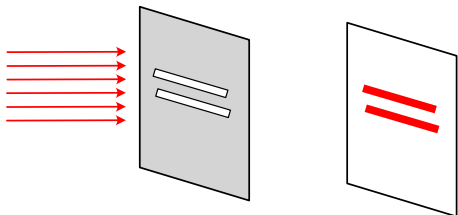
~600

540 **Figure 2.** Comparison of different approaches to imaging. (b) represents the truth and contains
 541 11.0 million pieces of information (assumed unavailable in the example). (a) is a version of (b)
 542 that is blurry due to smoothing by a factor of 70 in both directions, resulting in ~2300 pieces of
 543 information. (c) is an image constructed out of cow features (head, udder, legs, spots, eyes,
 544 ears, tag) and uses ~600 pieces of information. The smoothed image in (a) is most useful in
 545 discovery mode. The featured image in (c) is most useful in inference mode.

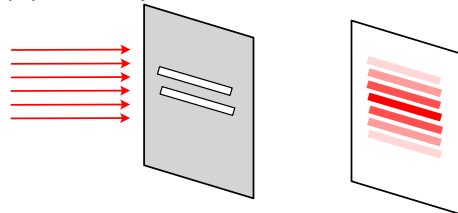
546

547

(a) Classical particle prediction



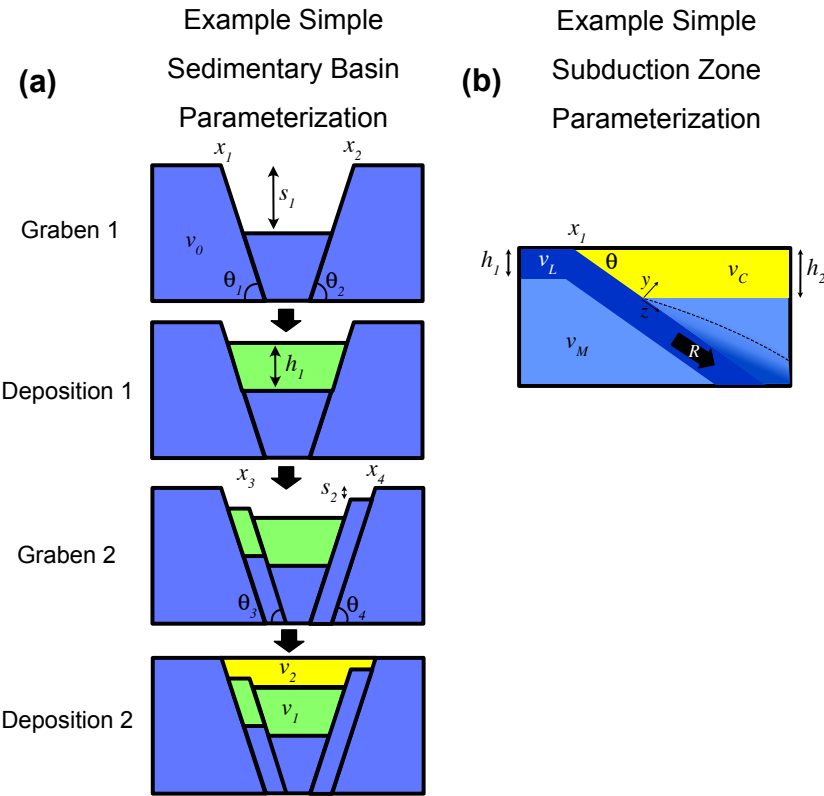
(b) Wave prediction



548

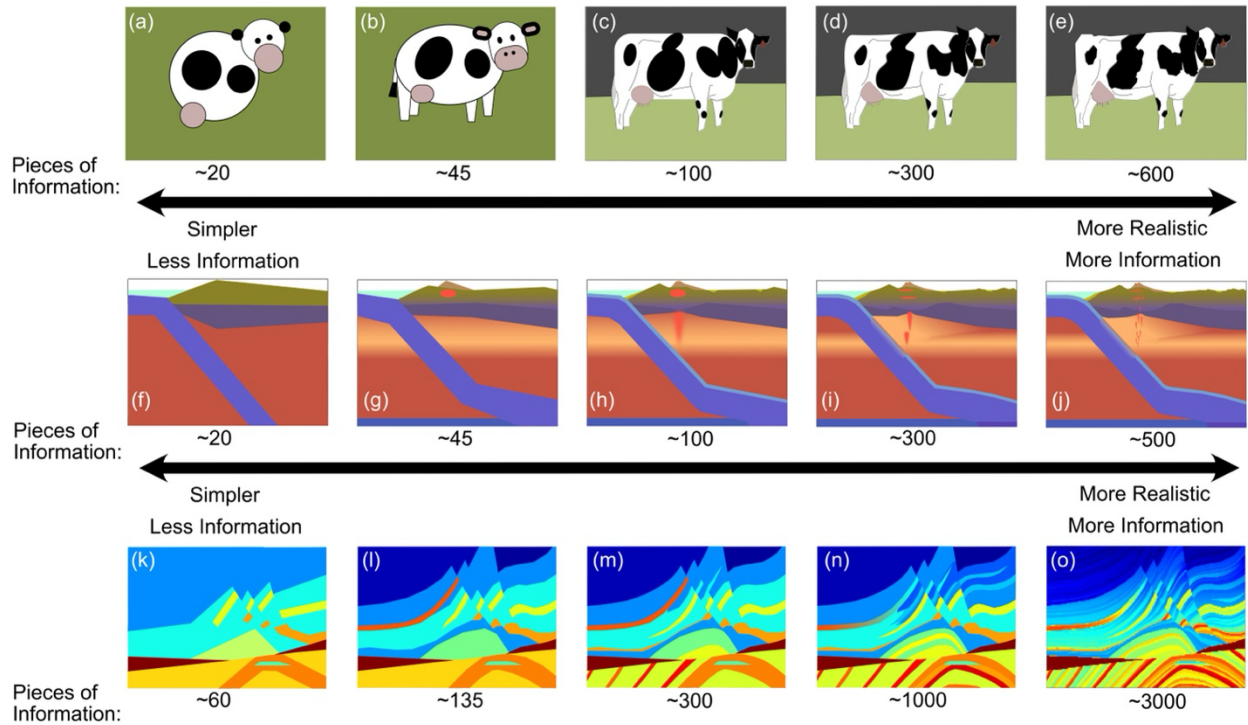
549 **Figure 3.** Young's double slit experiment with 2 distinct imaging hypotheses. (a) The classical
550 theory predicts 2 lines. (b) The wave theory predicts a central peak and a large number of
551 adjacent lines of different intensities depending on the wavelength. The purpose of the
552 experiment is to test the 2 specific hypotheses.

553



554

555 **Figure 4.** Example geologic parametrizations for imaging. (a) Example sedimentary basin
 556 parametrization with 14 parameters, characterizing 2 graben forming and 2 deposition geologic
 557 events. (b) Example subduction zone parametrization with 8 parameters, including cooling of
 558 the mantle wedge by the subducting plate. Adapted from Tsai et al. (2023).
 559



560

561 **Figure 5.** Schematic showing how models of a cow (a-e), a subduction zone (f-j) and a shallow
 562 subsurface structure (k-o) can be simpler or more realistic and encode less information or more
 563 information, respectively. The approximate number of pieces of information required to
 564 produce the cartoon in each panel is provided below each image. (a) A 'spherical cow' cartoon.
 565 (b-d) Intermediate complexity cartoon cows. (e) A realistic cartoon cow that approximates the
 566 cow in Fig. 2b. The geologic models in (f-o) are not just composed of arbitrary geometric objects
 567 but instead represent various geophysical processes and assumed deformation rules when used
 568 for 'geological tomography'. Structure in (k-o) inspired by the Marmousi model (Bourgeois et
 569 al., 1990).

570